Interpolyelectrolyte Complexes of Anionic Water-Soluble Conjugated Polymers and Proteins as Platforms for Multicolor Protein Sensing and Quantification

Dingyi Yu, Yong Zhang, and Bin Liu*

Department of Chemical and Biomolecular Engineering, National University of Singapore, 4 Engineering Drive 4, Singapore 117576, Singapore

Received January 12, 2008; Revised Manuscript Received March 18, 2008

ABSTRACT: A simple method for protein detection and quantification has been developed by taking advantage of the aggregation-induced fluorescence change of anionic water-soluble conjugated polymers. These polymers contain charged carboxylate groups and a π-electron delocalized optically active backbone composed of fluorene segments and 2,1,3-benzothiadiazole (BT) units. The polymers were synthesized through the Suzuki coupling between 2,7-[bis(4,4,5,5-tetramethyl-1,3,2-dioxaborolan-2-yl)-9,9-bis(3-(*tert*-butyl propanoate))]fluorene, 2,7-dibromo-9,9-bis(3′-(*tert*-butylpropanoate))fluorene, and 4,7-dibromo-2,1,3-benzothiadiazole, which was followed by treatment in trifluoroacetic acid to afford the functional carboxylic acid groups. **P1-BT$_x$** and **P2-BT$_x$** refer to the neutral precursor polymers and the anionic water-soluble polymers, respectively. The subscript in **P1-BT$_x$** and **P2-BT$_x$** (x = 7.5, 15, 30) refers to the molar percentage of BT units in the polymer backbone, which is 7.5%, 15%, and 30%, respectively. Both the optical spectra and the light scattering studies show that the polymers are aggregated in water at low pH, and the aggregation decreases at high pH. Along with the aggregation and aggregation breakup processes, the polymer emission also changes from yellow to blue in solution. At pH > 9, where most carboxylic acid groups are deprotonated, intense blue fluorescence is observed for all three polymer solutions. Using **P2-BT$_{30}$** as an example, addition of proteins to the polymer solution results in a change of emission color from blue to yellow, green, and dark for lysozyme, bovine serum albumin, and cytochrome *c*, respectively. The color change is due to efficient intramolecular/intermolecular energy transfer from the fluorene segments to the BT sites or electron transfer between the polymer and proteins upon complex formation. The variation in polymer emission color in the presence of different proteins is due to the difference in hydrophobic nature, net charge, and the structure among proteins. As demonstrated with **P2-BT$_{30}$** and lysozyme, the protein-induced polymer emission change has also been used to quantify protein concentrations.

Introduction

Conjugated polymers (CPs) coordinate the action of a large number of optically active absorbing units with delocalized electronic structures that allow for electronic coupling between optoelectronic segments and efficient intra- and interchain energy transfer.[1] Important properties of conjugated polymers, such as charge transport,[2] conductivity,[3] emission intensity,[4] and exciton migration,[2] are easily perturbed by external agents, leading to substantial changes in measurable signals.[5] Careful incorporation of anionic or cationic functionalities into conjugated polymers yield new materials that possess the beneficial properties of conjugated polymers with aqueous solubility for biosensor applications.[6,7] These water-soluble CPs have been used as light-harvesting molecules that deliver excitations to signaling fluorescent dyes attached to biomolecular probes, thereby providing increased signal intensities and sensitivities over those of single molecule reporters.[8] CP-based sensors that operate on fluorescence resonance energy transfer (FRET) mechanisms have been widely used to detect nucleic acids, small molecules, and proteins in solution and on solid substrate.[1i,j,9]

Complex formation between CPs and biomolecules through electrostatic interaction or specific "lock−key" recognition generally results in polymer aggregation and fluorescence quenching.[4,6c,10] Polymer aggregation is not a desirable process for many applications, and only few chemical and biological sensors took advantage of aggregation of conjugated polymers.[1j,11] In our previous studies, a cationic conjugated polymer, poly[9,9-bis(6′-*N*,*N*,*N*-trimethylammonium bromide) hexyl)fluorene-*co*-1,4-phenylene-*co*-4,7-(2,1,3-benzothiadiazole)], containing a fractional substitution of fluorene fragments with 2,1,3-benzothiadiazole (BT) units, was designed to facilitate multiple color DNA assays.[1j] The working hypothesis is that FRET from the phenylene−fluorene segments to the BT sites occurs more efficiently via interchain contacts in aggregation than that via the intrachain process within more isolated polymer chains. In dilute solutions, the polymer emits in the blue region. Complex formation between the polymer and an oppositely charged DNA molecule gives rise to polymer aggregation, which increases the local concentration of BT units, leading to increased interchain contacts and improved electronic coupling between optical partners. Under these conditions, energy transfer between the fluorene−phenylene units to the BT sites is more efficient than that for isolated chains, and green emission dominates the solution fluorescence. The aggregation-induced blue-to-green solution fluorescence change of BT-containing polymers was subsequently used for DNA concentration determination and enzyme activity study.[11d,12] Recently, an anionic poly(*p*-phenylene ethynylene) (PPE) containing green-emitting excition trap sites was also reported to detect biologically relevant amines based on the aggregation-enhanced exciton migrations to induce a blue-green fluorescence change.[2c]

Interpolyelectrolyte aggregation is often observed upon polymer interaction with different proteins.[13,14] The protein binding-induced conformational change of conjugated polyelectrolyte could result in modified fluorescence properties of conjugated polyelectrolyte. Previous studies showed that conjugated polyelectrolyte was not very selective to proteins.[13a,b,14] The nonspecific interaction of a carboxylate-substituted PPE with different proteins was reported as a cautionary tale for biosensor applications.[14] Our recent studies have shown that

* Corresponding author. E-mail: cheliub@nus.edu.sg.

10.1021/ma800082k CCC: $40.75
Published on Web 05/15/2008

the fluorescence of a carboxylic acid functionalized polyfluorene could be quenched to various degrees by proteins, such as cytochrome *c* (cyt *c*), lysozyme, myoglobin, and bovine serum albumin (BSA).[15a] This observation is similar to the previous report that a sulfonated PPV could be strongly quenched by cyt *c*, but to less extent by lysozyme and myoglobin.[10a] The response of conjugated polymers to different proteins is reflected by the difference in Stern−Volmer quenching constants, which is not convenient for protein detection. In a recent study, six functionalized PPEs have been used to build a protein sensor array.[16] Because of the difference in charge characteristics and molecular scales, these polymers provide binding diversity upon interaction with protein analytes, generating distinct fluorescence response pattern for protein discrimination. Although this method is proved to be effective for protein detection with high accuracy (97%), it functions on fluorescence quenching of polymers and requires multiple titration processes. It is highly desirable that a fluorescence turn-on or colorimetric sensor could be developed using a single polymer which could respond to different proteins with high selectivity and high accuracy.

The key challenge for the development of effective protein sensors is the creation of materials featuring appropriate surface areas for binding protein exteriors, coupled with the control of structure and functionality required for selectivity.[16] The second challenge in protein sensing is the signal transduction of the binding event. Water-soluble conjugated polymers containing low-energy traps in the backbone with pendant charged residues could provide an excellent scaffold for sensor design. These materials can bind protein surface through multivalent interactions. Upon binding, the aggregation-induced intensity and emission color change of polymers could be used to report the binding event. By adjusting pH of the media, both charge density and the nature of the charge could be fine-tuned for proteins and carboxylic acid functionalized polymers to optimize their mutual interactions.[15a] On the basis of the operation principle we and others demonstrated for multicolor target detection,[1j,2c] it occurred to us that we could take advantage of polymer aggregation on protein surface to achieve multicolor protein sensing.

In this contribution, we report the design and synthesis of anionic BT-containing polymers for multicolor protein detection and quantification. We start with the synthesis of polyfluorene copolymers containing different amount of BT units within the polymer backbone and study the intrinsic optical properties of these new materials under different experimental conditions. We then examine the perturbation in polymer emission properties upon interaction with different proteins and show how these interactions lead to changes in energy transfer within the polymers and charge transfer/energy transfer between the polymers and the proteins. Using **P2-BT$_{30}$** and lysozyme protein as an example, we also show that the protein-induced polymer emission change could be used to quantify protein concentrations.

Experimental Section

Materials. 2,7-Dibromofluorene was purchased from Aldrich. The monomers 2,7-dibromo-9,9-bis(3′-(*tert*-butylpropanoate))fluorene (**1**),[15a] 2,7-bis(4,4,5,5-tetramethyl-1,3,2-dioxaborolan-2-yl)-9,9-bis(3′-(*tert*-butylpropanoate))fluorene (**2**),[15a] and 4,7-dibromo-2,1,3-benzothiadiazole (**3**)[1j] were synthesized according to the previous literatures. Other reagents were used as received from Aldrich or Acros without further purification. Mill-Q water (18.2 MΩ) was used to prepare all polymer solutions.

Instrumentation. The ^{1}H NMR and ^{13}C NMR spectra were taken on a Burker 300 MHz spectrometer. UV−vis absorption spectra were collected with a Shimadzu UV-1700 spectrophotometer. Fluorescence was measured using a Perkin-Elmer LS-55 equipped with a xenon lamp excitation source and a Hamamatsu (Japan) 928 PMT, using 90° angle detection for solution samples. The solution pH was measured using a pH meter (Sartorius PB-10) with a glass/reference electrode, calibrated with buffers of pH = 4, 7, and 10. GPC analysis was conducted at 35 °C using a Waters 2690 liquid chromatography system equipped with a Waters 996 photodiode detector. Polystyrenes were used as the standard, and tetrahydrofuran (THF) was used as the eluent at a flow rate of 1.0 mL/min. Light scattering data were collected with a laser light scattering (LLS) 90 Plus (Brookhaven Instrument Corp.) at 24 ± 1 °C.

General Synthetic Procedures for BT-Containing Polymers. *Poly[9,9-bis(3′-(tert-butyl propanoate))fluorene-co-4,7-(2,1,3-benzothiadiazole)$_{7.5}$] (***P1-BT$_{7.5}$***).* Monomer **1** (247 mg, 0.425 mmol), monomer **2** (337 mg, 0.50 mmol), monomer **3** (22 mg, 0.075 mmol), $Pd(Ph_3P)_4$ (8 mg), and potassium carbonate (830 mg, 6 mmol) were placed in a 25 mL round-bottom flask. A mixture of water (3 mL) and toluene (9 mL) was added to the flask, and the reaction vessel was degassed. The mixture was heated at 90 °C for 24 h under argon and then precipitated into methanol. The polymer was filtered and washed with methanol and acetone and then dried under vacuum overnight to afford the neutral polymer **P1-BT$_{7.5}$** (300 mg, 75%) as a yellow fibrous solid. ^{1}H NMR (300 MHz, $CDCl_3$) δ (ppm): 8.16 (br, 0.15H), 7.73−7.85 (br, 6H), 2.53 (br, 4H), 1.65 (br, 4H), 1.30 (s, 18H). ^{13}C NMR (75 MHz, $CDCl_3$) δ (ppm): 173.17, 154.68, 149.67, 141.08, 137.43, 133.76, 132.50, 129.62, 127.4.3, 122.04, 120.80, 80.48, 54.43, 35.14, 30.58, 28.42.

*Poly[9,9-bis(3′-(tert-butyl propanoate))fluorene-co-4,7-(2,1,3-benzothiadiazole)$_{15}$] (***P1-BT$_{15}$***).* Monomer **1** (203 mg, 0.35 mmol), monomer **2** (337 mg, 0.50 mmol), monomer **3** (44 mg, 0.15 mmol), $Pd(Ph_3P)_4$ (8 mg), and potassium carbonate (830 mg, 6 mmol) were placed in a 25 mL round-bottom flask. A mixture of water (3 mL) and toluene (9 mL) was added to the flask, and the reaction vessel was degassed. The mixture was heated at 90 °C for 24 h under argon and then precipitated into methanol. The polymer was filtered and washed with methanol and acetone and then dried under vacuum overnight to afford the neutral polymer **P1-BT$_{15}$** (270 mg, 70%) as a yellow fibrous solid. ^{1}H NMR (300 MHz, $CDCl_3$) δ (ppm): 8.17 (br, 0.28H), 7.72−7.85 (br, 6H), 2.53 (br, 4H), 1.65 (br, 4H), 1.31 (s, 18H). ^{13}C NMR (75 MHz, $CDCl_3$) δ (ppm): 173.17, 154.68, 149.67, 141.10, 137.18, 133.75, 131.30, 129.59, 128.51, 124.45, 120.80, 80.48, 54.44, 35.13, 30.59, 28.40.

*Poly[9,9-bis(3′-(tert-butyl propanoate))fluorene-co-4,7-(2,1,3-benzothiadiazole)$_{30}$] (***P1-BT$_{30}$***).* Monomer **1** (116 mg, 0.20 mmol), monomer **2** (337 mg, 0.50 mmol), monomer **3** (88 mg, 0.30 mmol), $Pd(Ph_3P)_4$ (8 mg), and potassium carbonate (830 mg, 6 mmol) were placed in a 25 mL round-bottom flask. A mixture of water (3 mL) and toluene (9 mL) was added to the flask, and the reaction vessel was degassed. The mixture was heated at 90 °C for 24 h under argon and then precipitated into methanol. The polymer was filtered and washed with methanol and acetone and then dried under vacuum overnight to afford the neutral polymer **P1-BT$_{30}$** (220 mg, 65%) as a yellow fibrous solid. ^{1}H NMR (300 MHz, $CDCl_3$) δ (ppm): 8.17 (br, 0.60H), 7.72−8.02 (br, 6H), 2.55 (br, 4H), 1.75 (br, 4H), 1.31 (s, 18H). ^{13}C NMR (75 MHz, $CDCl_3$) δ (ppm): 173.24, 154.68, 149.63, 141.36, 137.43, 133.76, 132.50, 129.62, 128.56, 124.49, 120.73, 80.50, 54.45, 35.08, 30.77, 28.40.

*Poly[9,9-bis(3′-propanoate)fluorene-co-4,7-(2,1,3-benzothiadiazole)$_{7.5}$] Sodium Salt (***P2-BT$_{7.5}$***).* **P1-BT$_{7.5}$** (100 mg) was dissolved in dichloromethane (25 mL) in a 50 mL flask. After addition of trifluoroacetic acid (3 mL), the mixture was stirred for 4 h at room temperature. After removal of the solvent, the yellow-greenish residue was treated with Na_2CO_3 aqueous solution (0.10 M, 30 mL) at room temperature overnight. The polymer was purified through dialysis against Mill-Q water (M_w cutoff: 3500) for 3 days. The solution was freeze-dried to give **P2-BT$_{7.5}$** (75 mg, 90%) as a yellow solid. ^{1}H NMR (300 MHz, CD_3OD) δ (ppm): 8.19 (m, 0.15H), 7.87−7.98 (m, 6H), 2.58 (br, 4H), 1.51 (br, 4H).

*Poly[9,9-bis(3′-propanoate)fluorene-co-4,7-(2,1,3-benzothiadiazole)$_{15}$] sodium salt (***P2-BT$_{15}$***).* **P1-BT$_{15}$** (100 mg) was dissolved in dichloromethane (25 mL) in a 50 mL flask. After addition of trifluoroacetic acid (3 mL), the mixture was stirred for 4 h at room temperature. After removal of the solvent, the yellow-greenish

Scheme 1. Synthetic Route to the Polymers of P1-BT$_x$ and P2-BT$_x$

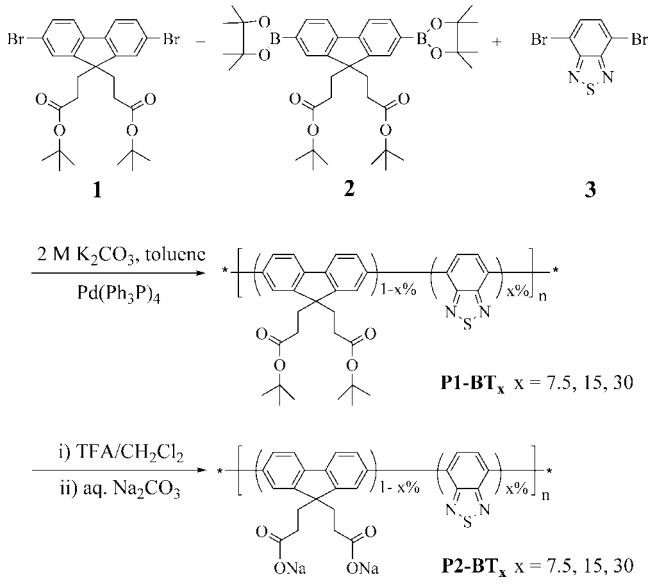

residue was treated with Na_2CO_3 aqueous solution (0.10 M, 30 mL) at room temperature overnight. The polymer was purified through dialysis against Mill-Q water (M_w cutoff: 3500) for 3 days. The solution was freeze-dried to give **P2-BT$_{15}$** (80 mg, 94%) as a yellow solid. ^{1}H NMR (300 MHz, CD_3OD) δ (ppm): 8.19 (m, 0.28H), 7.87−7.99 (m, 6H), 2.55 (br, 4H), 1.51 (br, 4H).

*Poly[9,9-bis(3′-propanoate)fluorene-co-4,7-(2,1,3-benzothiadiazole)$_{30}$] Sodium Salt (***P2-BT$_{30}$***).* **P1-BT$_{30}$** (100 mg) was dissolved in dichloromethane (25 mL) in a 50 mL flask. After addition of trifluoroacetic acid (3 mL), the mixture was stirred for 4 h at room temperature. After removal of the solvent, the yellow-greenish residue was treated with Na_2CO_3 aqueous solution (0.10 M, 30 mL) at room temperature overnight. The polymer was purified through dialysis against Mill-Q water (M_w cutoff: 3500) for 3 days. The solution was freeze-dried to give **P2-BT$_{30}$** (80 mg, 93%) as an orange solid. ^{1}H NMR (300 MHz, CD_3OD) δ (ppm): 8.22 (m, 0.59H), 7.89−8.00 (m, 6H), 2.60 (br, 4H), 1.58 (br, 4H).

Results and Discussion

Synthesis and Characterization. To synthesize anionic water-soluble BT containing polymers, we have chosen *tert*-butyl propanoate as the side chain of polyfluorene to maintain good solubility of the neutral precursor polymer and to reduce the hydrophobic component of the side chain after deprotection.[17] The development of a key intermediate, 2,7-bis(4,4,5,5-tetramethyl-1,3,2-dioxaborolan-2-yl)-9,9-bis(3-(*tert*-butyl propanoate)) fluorene,[15a] allows us to synthesize anionic water-soluble polymers that only contain fluorene and BT units in the polymer backbone with fully carboxylate functionalized side chains. With each fluorene ring containing two carboxylate groups, the high charge density would lead to good water solubility of the synthesized polymers.

The synthetic entry to the polymers is shown in Scheme 1. The monomers 2,7-dibromo-9,9-bis(3′-(*tert*-butylpropanoate)) fluorene (**1**), 2,7-bis(4,4,5,5-tetramethyl-1,3,2-dioxaborolan- 2-yl)-9,9-bis(3′-(*tert*-butylpropanoate))fluorene (**2**), and 4,7-dibromo-2,1,3-benzothiadiazole (**3**) were synthesized according to the previous reports.[1j,15a] Direct alkylation of 2,7-dibromofluorene using *tert*-butyl acrylate in a mixture of toluene/aqueous KOH gave monomer **1** in 51% yield. Conversion of **1** to the diboronic ester **2** was achieved under the Miyaura reaction conditions in the presence of bis(pinacolato)diborane, $Pd(dppf)_2Cl_2$, and KOAc using dry dimethylformamide (DMF) as the solvent. Monomer **2** was obtained in 93% yield after purification by silica column chromatography. Monomer **3** was synthesized in 60% yield by refluxing 2,1,3-benzothiadiazole in 47% HBr solution upon addition of bromine.[1j] The structure and purity of **1**, **2**, and **3** were confirmed with NMR and MS spectroscopies and elemental analysis.[18]

To obtain two emission colors from a single polymer chain, different amounts of BT units are introduced into the polyfluorene backbone. The synthetic approach involves a Suzuki copolymerization of **2** with a mixture of **1** and **3** to afford the neutral polymers of **P1-BT$_x$.** The subscript "x" refers to the molar percentage of BT units in these polymers, while (1 − x%) corresponds to the fraction of the fluorene segments. In Scheme 1, x = 7.5, 15, and 30 refer to the molar percentage of BT units in the polymer backbone, which are 7.5%, 15%, and 30%, respectively. The obtained neutral polymers **P1-BT$_x$** are soluble in organic solvents such as dichloromethane, toluene, and THF and can be easily purified by repeated precipitation from toluene solutions into methanol. The NMR spectroscopies confirmed the right structures and high purity of **P1-BT$_x$.** Molecular weight measured by GPC analysis against polystyrene standards shows the weight-average molecular weight (M_w) for **P1-BT$_{7.5}$, P1-BT$_{15}$**, and **P1-BT$_{30}$** is 9300, 11 000, and 11 000, respectively, with a polydispersity of 1.7, 1.9, and 1.8. In a second step, hydrolysis of the ester groups of **P1-BT$_x$** occurs in a mixture of CH_2Cl_2 and trifluoroacetic acid (TFA) (v/v = 1/1) at room temperature. After solvent evaporation, the residue is treated with aqueous Na_2CO_3 (0.1 M). The target polymers are then purified by dialysis against Mill-Q water using a 3.5 kDa molecular weight cutoff dialysis membrane for 3 days. After freeze-drying, the anionic polymers of **P2-BT$_x$** are obtained in a yield of ∼60%. The polymers of **P2-BT$_x$** are soluble in polar solvents, such as DMF, methanol, and H_2O. In the ^{1}H NMR spectra of **P2-BT$_x$,** there is no residual peak observed at ∼1.31 ppm that corresponds to −COOC(CH_3)$_3$ in **P1-BT$_x$**, which indicates that over 95% of −COOC(CH_3)$_3$ is converted to −COONa. From the ratio of integrated peaks (∼8.2 ppm for protons of BT units vs 7.7−7.9 ppm for aromatic protons of fluorene segments), the content of BT units within **P2-BT$_x$** is estimated to be 7.5%, 14.0%, and 29.5% for **P2-BT$_{7.5}$**, **P2-BT$_{15}$**, and **P2-BT$_{30}$**, respectively. The solubility of **P2-BT$_x$** in Milli-Q water (pH = ∼6) decreases with increased BT contents in the polymer backbone, which is measured to be ∼2.0, 0.8, and 0.1 mg/mL for **P2-BT$_{7.5}$**, **P2-BT$_{15}$**, and **P2-BT$_{30}$**, respectively.

pH-Dependent Aggregation of P2-BT$_x$. The degree of polymer aggregation in water at different pH was monitored by laser light scattering (LLS) techniques. LLS results in Figure 1 show the pH effect on the effective diameter (ED) for **P2-BT$_x$** aqueous solutions at [RU] = 2.0×10^{-5} M. Here RU refers to the average polymer repeat unit.[19] At pH > 5, the EDs of **P2-BT$_x$** are in the range of 100−300 nm. The data shown in Figure 1 are the average of three measurements, with ±10% errors. As the pH decreases, all polymers show a sudden increase in ED at pH = 4 to 3. At pH = 3, the EDs for all polymers are close to 2000 nm. Obvious precipitation is observed at pH = 2, and the solutions appear cloudy for all polymers. These data indicate the substantial polymer chain aggregation upon protonation of the pendent groups. Protonation of the carboxylic acid groups at low pH renders the polymers charge neutral which leads to a decrease in interchain electrostatic repulsion and favors polymer aggregation. At pH < 3, the polymers should be mainly in the protonated state. At pH > 10, most of the side chains in **P2-BT$_x$** should be negatively charged, and the repulsion between negative charges leads to extended polymer structures in solution.

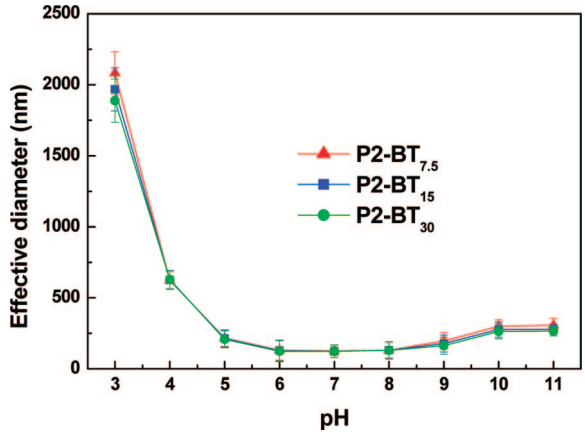

Figure 1. Effective diameters (EDs) determined by laser light scattering of **P2-BT$_{7.5}$**, **P2-BT$_{15}$**, and **P2-BT$_{30}$** ([RU] = 2.0 × 10^{-5} M) in water as a function of pH.

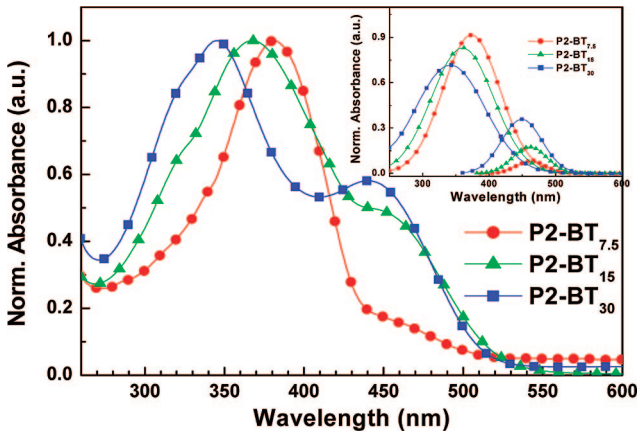

Figure 2. Normalized absorption spectra of **P2-BT$_{7.5}$**, **P2-BT$_{15}$**, and **P2-BT$_{30}$** in water. The inset shows the deconvoluted absorption spectrum for each polymer.

Absorption and Photoluminescence Spectra of P2-BT$_x$. Figure 2 shows the normalized absorption spectra of **P2-BT$_x$** ([RU] = 1.0 × 10^{-6} M) in Milli-Q water (pH = ~6). For each polymer, the absorption spectrum displays two bands at ~300−400 and ~400−500 nm, respectively. The band at ~300−400 nm is assigned to the $\pi-\pi^*$ transition for the fluorene segments, while the band located at ~400−500 nm is assigned to the BT sites.[20] The deconvoluted spectrum for each polymer is shown in the inset of Figure 2. As the fraction of BT in the backbone increases from 7.5% to 30%, one observes a concomitant increase in intensity of the ~400−500 nm absorption band and a decrease in intensity of the ~300−400 nm band. The intensity of the ~400−500 nm band for each polymer also agrees well with the feed ratio of the BT monomer during polymerization. In addition, with increased BT content in the polymer backbone, there is a blue shift observed for the fluorene segments. As shown in Figure 2, the maximum absorption peak that corresponds to the absorption of fluorene segments is 382 nm for **P2-BT$_{7.5}$**, 370 nm for **P2-BT$_{15}$**, and 345 nm for **P2-BT$_{30}$**. The blue shift is attributed to the decrease of effective conjugation length in **P2-BT$_x$** with increased amount of BT in the polymer backbone.[20] In methanol, the polymers have shown slightly blue-shifted absorption spectra with similar shapes as compared to those in water.

The photoluminescence (PL) spectra of **P2-BT$_x$** in water and in methanol are shown in parts a and b of Figure 3, respectively. The PL spectra are normalized with respect to the blue emission band for each polymer. As shown in Figure 3a, the PL spectra

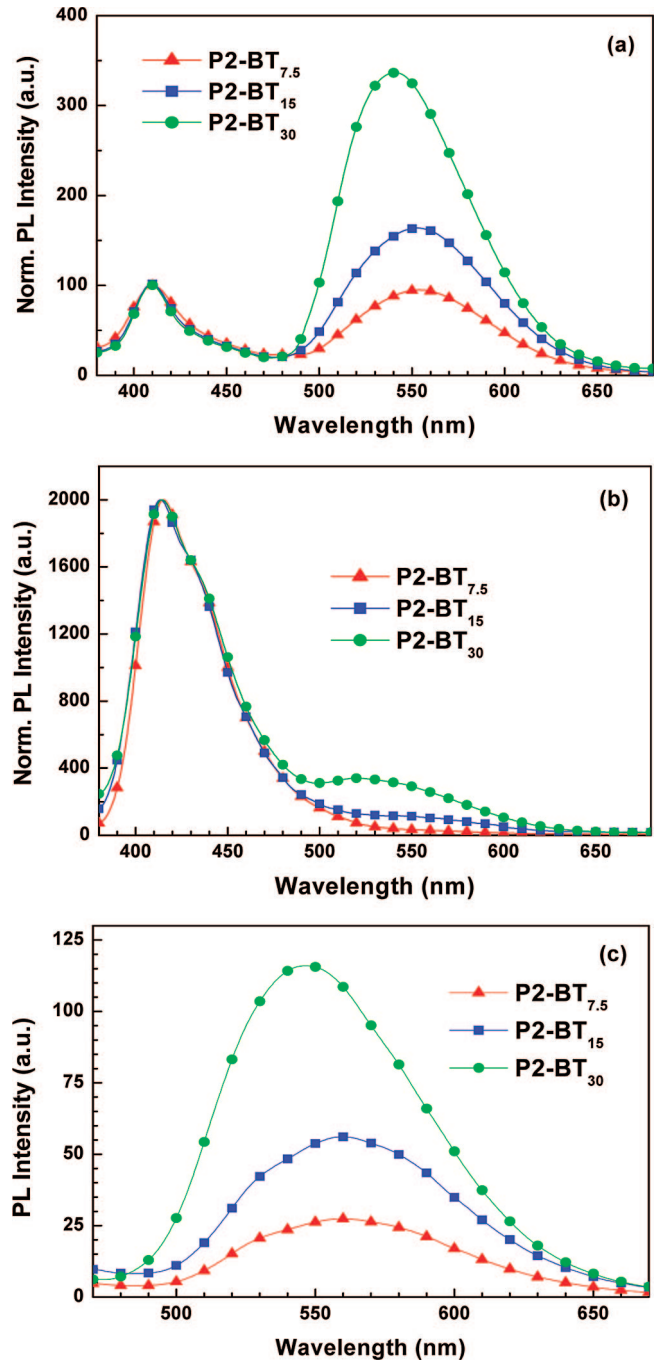

Figure 3. PL spectra of **P2-BT$_{7.5}$**, **P2-BT$_{15}$**, and **P2-BT$_{30}$** ([RU] = 1.0 × 10^{-6} M) in water (a) and in methanol (b). The excitation wavelength for **P2-BT$_{7.5}$**, **P2-BT$_{15}$**, and **P2-BT$_{30}$** is 382, 370, and 345 nm in water and 380, 367, and 345 nm in methanol, respectively. Direct excitation of BT at 450 nm for **P2-BT$_x$** in water is shown as (c).

of **P2-BT$_x$** in water (pH = 6) have two distinct peaks at 410 and 550 nm, and the emission is dominated by the BT emission band centered at 550 nm. The absolute intensity for the peak at 550 nm increases with the increased amount of BT in the polymer backbone. When excited at 450 nm, where preferential absorption by BT takes place, the intensity of the emission peaks that corresponds to **P2-BT$_{7.5}$**, **P2-BT$_{15}$**, and **P2-BT$_{30}$** ([RU] = 1.0 × 10^{-6} M) (Figure 3c) is proportional to the fractional composition of BT in the backbone. This result confirms again that the composition of polymers is similar to the feed ratio of the monomers during polymerization. As seen from Figure 3b, the PL spectra of **P2-BT$_x$** in methanol are dominated by blue emission, which are significantly different from those observed

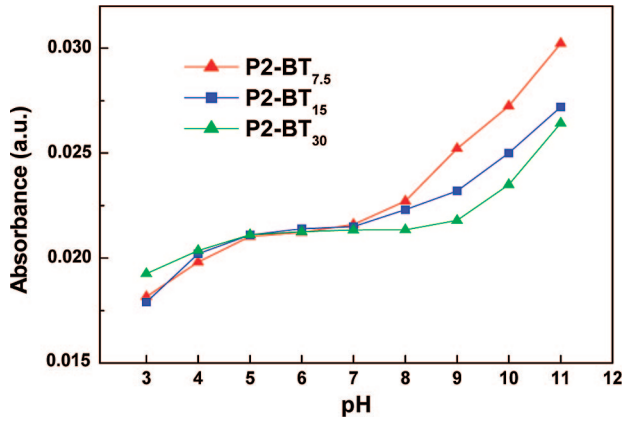

Figure 4. Dependence of polymer absorbance at the absorption maximum for **P2-BT$_{7.5}$**, **P2-BT$_{15}$**, and **P2-BT$_{30}$** on pH ([RU] = 1.0×10^{-6} M) in water.

in water. In methanol, the emission intensity at ~550 nm also decreases for each polymer as compared to that in water, and there is almost no BT emission band observed for **P2-BT$_{7.5}$**. The decrease of the long-wavelength emission in methanol compared to that in water is due to less aggregation of **P2-BT$_x$** in methanol, which reduces intermolecular energy transfer from the fluorene segments to the BT units.[20] For **P2-BT$_{7.5}$**, the PL spectrum in methanol is very similar to hydrophobic polyfluorenes (i.e., poly(9,9-dihexylfluorene)) in good solvents, such as chloroform, indicating that the aggregation of **P2-BT$_{7.5}$** is minimum in methanol.[21] For **P2-BT$_{15}$** and **P2-BT$_{30}$**, because of the large fractional component of BT units in polymer backbone, it is possible that both intermolecular and intramolecular energy transfer contribute to the BT emission in methanol. The difference in BT emission in water and methanol is consistent with the idea that less efficient energy transfer between the fluorene segments and the BT units occurs in isolated chains, relative to situations where interchain energy transfer is favorable.

pH Effect on Absorption and Photoluminescence Spectra of P2-BT$_x$. The absorption of **P2-BT$_{7.5}$**, **P2-BT$_{15}$**, and **P2-BT$_{30}$** in Milli-Q water at pH = 3−11 was studied at [RU] = 1.0×10^{-6} M. The pH-dependent change of the maximum absorbance for each polymer is shown in Figure 4. For all polymers, there is about 30−40% increase in absorbance when pH is changed from 3 to 11. At pH = 3, the majority of the carboxylate groups are protonated and the polymers are mainly in the acid form. Charge neutralization decreases the interchain electrostatic repulsion and encourages interchain aggregation.[15b] In addition, low pH could favor hydrogen bonding between protonated carboxylic acid groups, which leads to more aggregated polymer states.[22] The low absorbance at pH = 3 is also supported by the LLS data, which is mainly due to aggregation and low solubility of the polymers in water. Similar aggregation-induced absorbance change was reported upon addition of various amounts of water to an anionic polyfluorene in methanol.[23] For all polymers, the absorbance at pH = 6 is nearly 10% higher than that at pH = 3, which indicates weaker interchain interactions (i.e., aggregation) at pH = 6 as compared to those at pH = 3. At pH = 11, deprotonation is a more favorable process. When most of the polymer chains are negatively charged, the polymer water-solubility increases. Repulsion between negatively charged carboxylate functionalities will cause the polymers to be in a less aggregated state. Therefore, the polymers have slightly higher absorbance at pH = 11 as compared to that at pH = 6. The difference in dissociation of the carboxylic acid groups at pH = 6 and 11 is also supported by the change in absorbance for n−π^* of −COOH. As shown in Figure S1 (Supporting Information), using **P2-BT$_{7.5}$** at [RU] = 1×10^{-6} M as an example, a peak centered at 217 nm is observed at pH = 6, which indicates that some −COOH groups remain in solution. The peak at ~217 nm almost disappears when pH is increased to 11, indicating that deprotonation increases with increased pH and the polymers are mainly in the deprotonated state at pH = 11. This observation is similar to the previous report for poly(isobutylene-*alt*-maleic acid) (PIM), which shows an absorption peak at 215 nm for −COOH at an ionization degree of 50%, and the peak disappears when PIM is fully ionized.[24]

Fluorescence changes of the polymer solutions upon varying the solution pH from 7 to 11 were also studied. The spectra are normalized with respect to the blue emission band to highlight the changes of the BT emission band under different pH. The results are shown in Figure 5. For **P2-BT$_x$**, the BT emission band gradually decreases with increasing pH. At pH = 11, when majority of the carboxylic aicd groups are deprotonated, there is virtually no obvious BT emission observed for all polymers. This observation indicates that at high pH the repelled polymer chains decrease the interchain interaction and greatly reduce the intermolecular energy transfer process. In addition, the extended polymer chains at high pH could further expose the BT units to the aqueous solution. The decrease in BT fluorescence at high pH is also constant with a charge-transfer excited state that increases its nonradiative decay rate in a more polar environment.[25] This charge transfer character was reported previously with a neutral BT containing polymer, where the BT emission was red-shifted ~10 nm upon addition of 10% of water to its THF solution.[26]

To verify that the chemical structure of BT is not affected by the change of solution pH, PL intensity of **P2-BT$_{30}$** ([RU] = 1.0×10^{-5} M) by cycling the pH between 3 and 10 was studied (Figure 6). In between each cycle, the polymer solution underwent dialysis against Milli-Q water to minimize the effect of ionic strength change (due to pH adjustment with HCl and NaOH) on polymer emission. The polymer solution was then calibrated against a solution of **P2-BT$_{30}$** with known concentration before fluorescence measurement. As shown in Figure 6, changes in BT emission intensity at 550 nm as a function of pH are reversible. These data indicate that protonation and deprotonation of the acid groups by changing the pH results in reversible aggregation.[26]

Salt Effect on Photoluminescence Spectra of P2-BT$_x$. For bioassay applications, it is highly desirable that the polymers could be stabilized in buffer solutions, since buffer ions are often used to maintain the solution pH and to screen the charges among biomolecules.[27] For protein detection, a buffer solution containing 5−150 mM ions is generally used. Under such ionic strength, previously reported water-soluble BT containing polymers underwent serious aggregation due to low charge density and low water solubility of the polymers.[12a] It is highly desirable that the polymers could have no or limited aggregation in buffer so that the emission change from target-induced polymer aggregation will not be interfered by polymer aggregation in the absence of the target. The emission spectra of **P2-BT$_{30}$** ([RU] = 1.0×10^{-6} M) in water as a function of [NaCl] are shown in Figure 7, and those for **P2-BT$_{7.5}$** and **P2-BT$_{15}$** are shown in Figures S2 and S3 (Supporting Information), respectively. For all polymers, there is a gradual decrease in BT emission and an increase in fluorene emission when [NaCl] is varied from 0 to 100 mM. This observation indicates that interchain/intrachain interaction decreases with increased ionic strength in solution. This behavior could be understood from the previous study of the ionic strength effect on pK_a of poly(carboxylic acid)s.[28] The presence of 100 mM NaCl can reduce the pK_a of poly(acrylic acid) from 6.17 to 5.11.[28] The

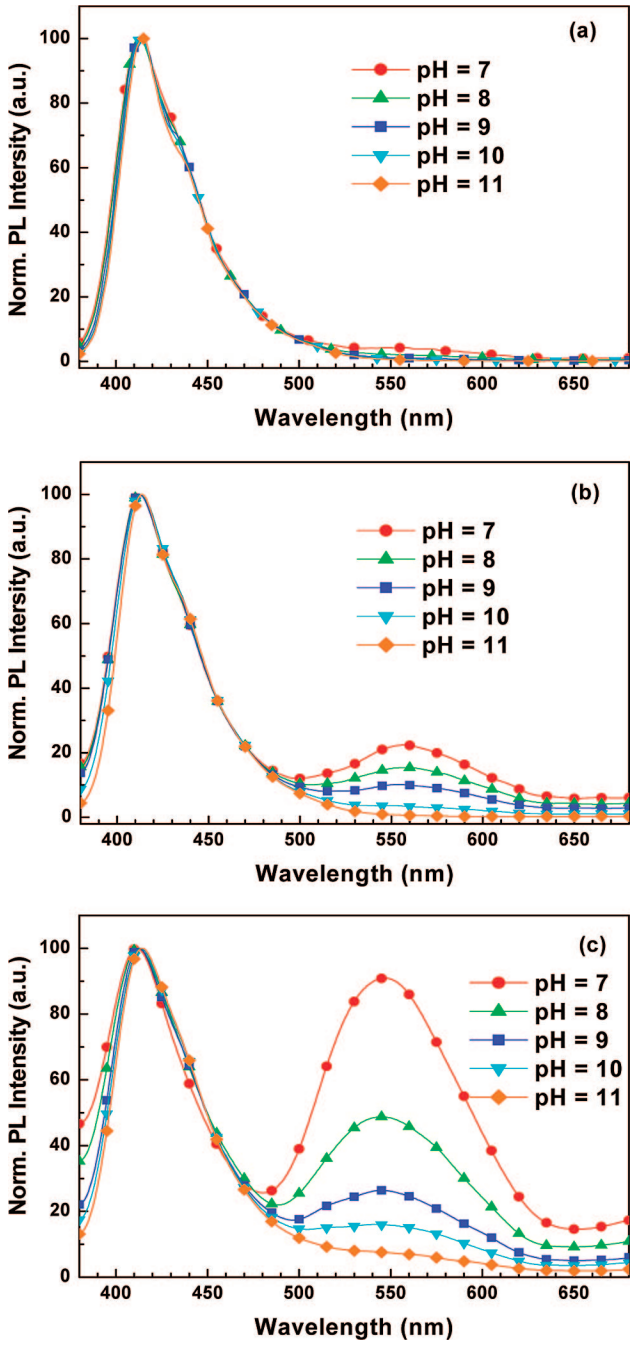

Figure 5. Photoluminescence (PL) spectra of **P2-BT$_{7.5}$** (a), **P2-BT$_{15}$** (b), and **P2-BT$_{30}$** (c) ([RU] = 1.0×10^{-6} M) in water as a function of pH. The excitation wavelength is the absorption maximum for each polymer.

presence of ions increases the shielding of the carboxyl group from the electrical effects of the nearby charged carboxylate groups, which favors the dissociation of protons from acid groups. As a consequence, the presence of NaCl increases the dissociation of the −COOH groups in **P2-BT$_x$**, which disfavors intrachain/interchain aggregation and results in less efficient energy transfer from the fluorene segments to the BT units. This assumption is supported by the decreased absorbance at 217 nm upon addition of NaCl to the solution of **P2-BT$_{7.5}$** as shown in Figure S4 (Supporting Information). On the other hand, upon addition of NaCl to the polymer solutions, the increased ionic strength could also cause polymer aggregation. This is evidenced by the decreased blue emission intensity upon addition of NaCl ([NaCl] > 100 mM) to polymer solutions (data not shown). For **P2-BT$_{30}$**, the BT emission tail could be suppressed by

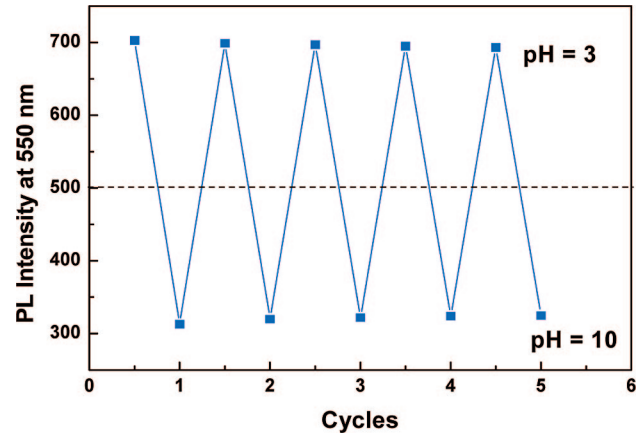

Figure 6. PL intensity of **P2-BT$_{30}$** ([RU] = 1.0×10^{-5} M) at 550 nm upon cycling the pH between 3 and 10.

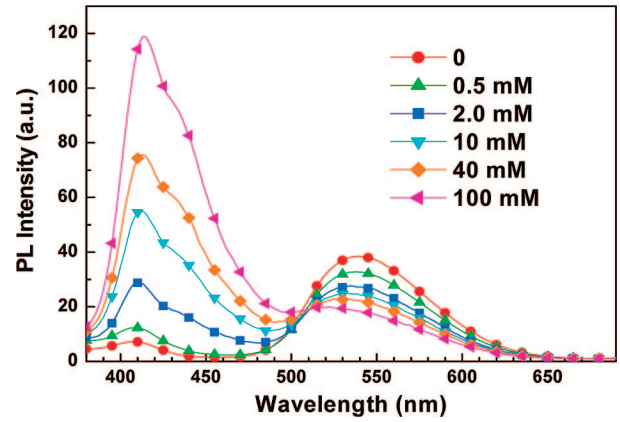

Figure 7. Changes of the PL spectra of **P2-BT$_{30}$** ([RU] = 1.0×10^{-6} M) as a function of [NaCl] in water.

increasing the solution pH and ionic strength simultaneously. At pH = 9, the presence of 25 mM NaCl in **P2-BT$_{30}$** solution yields no BT emission (Figure S5 in Supporting Information).

Photoluminescence Response to Different Proteins. Having established the emission profiles for **P2-BT$_x$** under different conditions provided us the opportunities to study the interactions of **P2-BT$_x$** with different proteins. Electrostatic and hydrophobic interactions between the polymers and different proteins should induce different degrees of polymer aggregation, leading to different patterns of polymer emission. The protein used in this study include cyt *c*, BSA, and lysozyme. Cyt *c* is a small heme protein found loosely associated with the inner membrane of the mitochondrion, which is capable of undergoing energy/electron transfer with conjugated polymers due to its metal center.[13c] BSA is one of the most widely studied proteins and is the most abundant protein in plasma.[29] Lysozyme is a ubiquitous bacteriolytic enzyme present in external secretions and in polymorphs and macrophages.[30] The isoelectric point (pI) of cyt *c*, BSA, and lysozyme proteins are 10.0, 4.9, and 11.0, respectively.[13c]

On the basis of the difference in BT emission intensity shown in Figures 3a for **P2-BT$_{7.5}$**, **P2-BT$_{15}$**, and **P2-BT$_{30}$** and the intense blue emission of **P2-BT$_{30}$** under optimized conditions (shown in Figure S5), it is obvious that **P2-BT$_{30}$** should give the most sensitive response to external disturbance. To reduce the background signal of BT emission, the medium of pH = 9 ([Na_2CO_3/$NaHCO_3$] = 2 mM) in the presence of 25 mM NaCl was selected (Figure S5 in Supporting Information). At pH = 9, cyt *c* and lysozyme are positively charged, while BSA is negatively charged. Because of the negatively charged nature

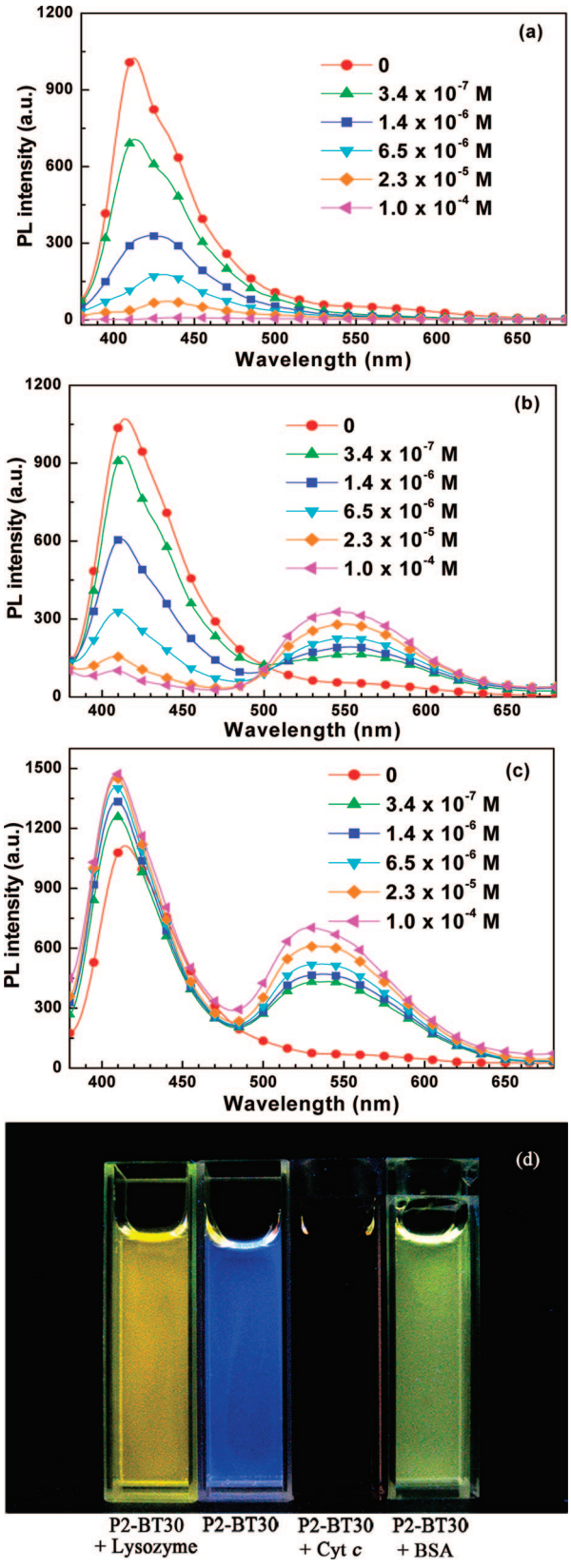

Figure 8. Changes in PL spectra of **P2-BT$_{30}$** ([RU] = 1.0×10^{-6} M) as a function of the concentration of (a) cyt *c*, (b) lysozyme, and (c) BSA in Na_2CO_3/$NaHCO_3$ buffer with [NaCl] = 25 mM (pH = 9.0). The excitation wavelength is the maximum absorption wavelength for each polymer. (d) Photographs for solutions of **P2-BT$_{30}$** in the presence of lysozyme, cyt *c*, and BSA under UV excitation (λ_{ex} = 365 nm).

of **P2-BT$_{30}$**, complex formation between the polymer and cyt *c* or lysozyme through electrostatic interactions is favorable. In addition, the hydrophobic driving force may also be cooperative, especially for the interaction between **P2-BT$_{30}$** and BSA.

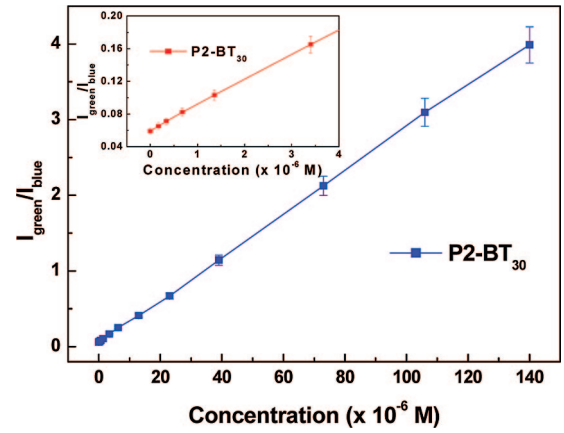

Figure 9. Ratios of I_{green}/I_{blue} for **P2-BT$_{30}$** ([RU] = 1.0×10^{-6} M) with respect to [lysozyme]. The inset shows the curve at low protein concentrations. The data are the average of three measurements.

Figure 8 compares the emission spectra of **P2-BT$_{30}$** upon addition of various amounts of lysozyme, BSA, and cyt *c* proteins, at the same concentration of [**RU**] = 1.0×10^{-6} M. The excitation wavelength is the maximum absorption wavelength for each polymer. Addition of cyt *c* to the polymer solution leads to significant quenching of the emission from fluorene segments at 410 nm, and there is no BT emission observed (Figure 8a). This is due to the metalloporphyrin functionality in cyt *c*, which is capable of quenching the excited state of **P2-BT$_{30}$**.[13c] In addition, the protein-induced aggregation of **P2-BT$_{30}$** should also affect its fluorescence quenching. To clarify the contribution of these two factors, lysozyme, a protein that does not contain any electron transfer center, is also used to interact with the polymer. As shown in Figure 8b, addition of lysozyme leads to quenching of the blue emission at 410 nm. Concomitant with the decrease in the blue region, there is a gradual increase in the BT emission band at 550 nm. This behavior is typical of the aggregation-induced energy transfer between the fluorene segments and the BT units, which is due to binding-induced polymer aggregation and increased interchain interaction. Addition of BSA to the polymer solution induces increase in emission for both fluorene segments and the BT units (Figure 8c). Since BSA is negatively charged at pH = 9, the surfactant nature of BSA tends to increase the polymer fluorescence.[14] In addition, hydrophobic interaction between the polymer and BSA causes increased interchain interactions among polymers on the protein surface, which favors energy transfer.

The difference in polymer response to proteins could thus be used to develop a colorimetric assay. Because of the different emission bands from **P2-BT$_{30}$** in extended and aggregated states, addition of BSA causes an increase in both blue and yellow bands. As a consequence, the emission appears green in color. For lysozyme, the emission color appears yellow since the addition of lysozyme causes quenching in the blue band but enhancement in the yellow band. Because of efficient electron transfer between cyt *c* and **P2-BT$_{30}$**, the polymer fluorescence is totally quenched, and the solution remains dark. Figure 8d shows the photographs of **P2-BT$_{30}$** in the presence of lysozyme, BSA, and cyt *c* proteins under excitation at 365 nm using a portable UV lamp. The distinguished color difference indicates the presence of different proteins in solution.

Protein Quantification. To obtain quantitative information on how the shift in emission color correlated to protein concentration, we added different amount of lysozyme to the

P2-BT$_{30}$ solution ([RU] = 1.0×10^{-6} M in 2 mM Na_2CO_3/$NaHCO_3$ buffer with 25 mM NaCl) to induce the polymer emission change. The ratios of the intensities for the BT and fluorene emission bands are calculated. As shown in Figure 9, when plotting the ratio as a function of the protein concentration, a linear curve is obtained for [lysozyme] varying from 0 to 140 μM. The curve that corresponds to the low protein concentration is enlarged in the inset of Figure 9. The detection limit for lysozyme is estimated to be 0.2 μM using a standard fluorometer. This sensitivity is close to other colorimetric assays for lysozyme detection using gold nanoparticles.[31] The linear relationship between the ratios of the emission intensity for two emission bands and lysozyme concentrations could also be used to quantify the lysozyme concentration in solution.

Conclusions

In summary, we report water-soluble carboxylated conjugated polymers that change emission color as a result of conformation and aggregation variations. The polymers were synthesized through the Suzuki coupling between carboxylate functionalized fluorene monomers and BT to afford the neutral polymers of **P1-BT$_x$**, which was followed by treatment in trifluoroacetic acid to afford the water-soluble polymers of **P2-BT$_x$**. The NMR data revealed the right contents of BT in **P2-BT$_x$** according to the feed ratio of BT during polymerization. Both the absorption and emission spectra showed that the polymers were aggregated in water at low pH and the aggregation decreased at high pH, which was supported by the light scattering data. Large aggregates (~2000 nm) were observed at pH = 3, while increasing the pH resulted in breakup of aggregates, as a result of electrostatic repulsion between the negatively charged polymer chains. Monitoring of the absorption spectra of −COOH revealed the presence of −COOH in solution at pH = 6, while the majority of the protons were dissociated form the carboxylic acid groups at pH = 11. The presence of NaCl was also found to favor the proton dissociation, which was evidenced by the decreased absorbance for −COOH upon addition of increased amount of NaCl to the **P2-BT$_{7.5}$** aqueous solution. Along with the deprotonation process, the polymer emission changed from yellow (pH < 6) to blue (pH > 9). Using **P2-BT$_{30}$** as an example, addition of proteins to the polymer solution resulted in emission spectral changes. Addition of lysozyme led to quenching of the blue emission band and a concomitant increase in the BT emission band. This behavior is typical to the aggregation-induced energy transfer, which is due to binding-induced polymer aggregation and increased interchain interaction. Addition of BSA to the polymer solution induced increase in emission for both fluorene segments and the BT units, which is due to the surfactant nature and the hydrophobic interaction between BSA and the polymer. Addition of cyt *c* to the polymer solution led to fluorescence quenching due to the metalloprotein which favors charge transfer. The net effect of the emission spectral variation is a change in emission color from blue to yellow, green, or dark for lysozyme, BSA, and cyt *c*, respectively. Using **P2-BT$_{30}$** and lysozyme protein as an example, we demonstrated that the protein-induced polymer emission change could be used to quantify protein concentrations, with a detection limit of 0.2 μM for lysozyme in solution. Further improvement of the water solubility and the BT content within the polymer could yield better polymers with higher detection sensitivity.

Acknowledgment. We are grateful to the National University of Singapore (NUS ARF R-279-000-197-112/133, R-279-000-233-123, YIA R-279-000-234-123, OLS R-279-000-212-712) and Singapore Ministry of Education (MOE R-279-000-255-112) for financial support.

Supporting Information Available: Absorption spectra of −COOH for **P2-BT$_{7.5}$** at different pH and in the presence of different amounts of NaCl; changes in photoluminescence spectra of **P2-BT$_{7.5}$** and **P2-BT$_{15}$** as a function of [NaCl] in water. This material is available free of charge via the Internet at http://pubs.acs.org.

References and Notes

(1) (a) Guillet, J. E. *Polymer Photophysics and Photochemistry*; Cambridge University Press: Cambridge, 1985. (b) Weber, S. E. *Chem. Rev.* **1990**, *90*, 1469–1482. (c) Kauffmann, H. F. *Photochemistry and Photophysics*; Radek, J. E., Ed.; CRC Press: Boca Raton, FL, 1990; Vol. 2. (d) Scholes, G. D.; Ghiggino, K. P. *J. Chem. Phys.* **1994**, *101*, 1251–1261. (e) Tasch, S.; List, E. J. W.; Hochfilzer, C.; Leising, G.; Schlichting, P.; Rohr, U.; Geerts, Y.; Scherf, U.; Müllen, K. *Phys. Rev. B* **1997**, *56*, 4479–4483. (f) Nguyen, T. Q.; Wu, J. J.; Doan, V.; Schwartz, B. J.; Tolbert, S. H. *Science* **2000**, *288*, 652–656. (g) Pschirer, N. G.; Byrd, K.; Bunz, U. H. F. *Macromolecules* **2001**, *34*, 8590–8592. (h) Beljonne, D.; Pourtois, G.; Silva, C.; Hennebicq, E.; Herz, L. M.; Friend, R. H.; Scholes, G. D.; Setayesh, S.; Müllen, K.; Brédas, J. L. *Proc. Natl. Acad. Sci. U.S.A.* **2002**, *99*, 10982–10987. (i) Liu, B.; Wang, S.; Bazan, G. C.; Mikhailovsky, A. *J. Am. Chem. Soc.* **2003**, *125*, 13306–13307. (j) Liu, B.; Bazan, G. C. *J. Am. Chem. Soc.* **2004**, *126*, 1942–1943. (k) Hennebicq, E.; Pourtois, G.; Scholes, G.; Herz, L.; Russell, D.; Silva, C.; Setayesh, S.; Grimsdale, A. C.; Müllen, K.; Brédas, J. L.; Beljonne, D. *J. Am. Chem. Soc.* **2005**, *127*, 4744–4762. (l) Thomas, S. W.; Joly, D. G.; Swager, T. W. *Chem. Rev.* **2007**, *107*, 1339–1386.

(2) (a) Lee, D. W.; Swager, T. M. *Synlett* **2004**, *149*, 154. (b) Kim, Y.; Bouffard, J.; Kooi, S. E.; Swager, T. M. *J. Am. Chem. Soc.* **2005**, *127*, 13726–13731. (c) Kim, Y.; Whitten, J. E.; Swager, T. M. *J. Am. Chem. Soc.* **2005**, *127*, 12122–12130. (d) Satrijo, A.; Swager, T. M. *J. Am. Chem. Soc.* **2007**, *129*, 16020–6028.

(3) (a) Korri, Y. H.; Garnier, F.; Srivastava, P.; Godillot, P.; Yassar, A. *J. Am. Chem. Soc.* **1997**, *119*, 7388–7389. (b) Bäuerle, P.; Emge, A. *Adv. Mater.* **1998**, *10*, 324–330. (c) Garnier, F.; Korri, Y. H.; Srivastava, P.; Mandrand, B.; Delair, T. *Synth. Met.* **1999**, *100*, 89–94. (d) Korri-Youssoufi, H.; Yassar, A. *Biomacromolecules* **2001**, *2*, 58–64.

(4) (a) Kumaraswamy, S.; Bergstedt, T.; Shi, X.; Rininsland, F.; Kushon, S.; Xia, W. S.; Ley, K.; Achyuthan, K.; McBranch, D.; Whitten, D. G. *Proc. Natl. Acad. U.S.A.* **2004**, *101*, 7511–7515. (b) Pinto, M. R.; Schanze, K. S. *Proc. Natl. Acad. U.S.A.* **2004**, *101*, 7505–7510.

(5) Swager, T. M. *Acc. Chem. Res.* **1998**, *31*, 201–207.

(6) (a) McQuade, D. T.; Pullen, A. E.; Swager, T. W. *Chem. Rev.* **2000**, *100*, 2537–2574. (b) Pinto, M. R.; Schanze, K. S. *Synthesis* **2002**, *1293*, 1309. (c) Chen, L.; McBranch, D. W.; Wang, H. L.; Helgeson, R.; Wudl, F.; Whitten, D. G. *Proc. Natl. Acad. U.S.A.* **1999**, *96*, 12287–12292. (d) Bazan, G. C. *J. Org. Chem.* **2007**, *72*, 8615–8635. (e) Huang, F.; Wang, X. H.; Wang, D. L.; Yang, W.; Cao, Y. *Polymer* **2005**, *46*, 12010–12015. (f) Wosnick, J. H.; Mello, C. M.; Swager, T. M. *J. Am. Chem. Soc.* **2005**, *127*, 3400–3405. (g) Traser, S.; Wittmeyer, P.; Rehahn, M. *e-Polym.* **2002**, 032.

(7) (a) Ho, H. A.; Boissinot, M.; Bergeron, M. G.; Corbeil, G.; Doré, K.; Boudreau, D.; Leclerc, M. *Angew. Chem., Int. Ed.* **2002**, *41*, 1548–1551. (b) Doré, K.; Dubus, S.; Ho, H. A.; Lévesque, I.; Brunette, M.; Corbeil, G.; Boissinot, M.; Boivin, G.; Bergeron, M. G.; Boudreau, D.; Leclerc, M. *J. Am. Chem. Soc.* **2004**, *126*, 4240–4244. (c) Ho, H. A.; Béra-Abérem, M.; Leclerc, M. *Chem.—Eur. J.* **2005**, *11*, 1718–1724. (d) Nilsson, K. P. R.; Inganäs, O. *Nat. Mater.* **2003**, *2*, 419–424. (e) Le Floch, F.; Ho, H. A.; Harding, L. P.; Bedard, M.; Neagu, P. R.; Leclerc, M. *Adv. Mater.* **2005**, *17*, 1251–1254. (f) Disney, M. D.; Zheng, J.; Swager, T. M.; Seeberger, P. H. *J. Am. Chem. Soc.* **2004**, *126*, 13343–13346.

(8) (a) Gaylord, B. S.; Heeger, A. J.; Bazan, G. C. *Proc. Natl. Acad. U.S.A.* **2002**, *99*, 10954–10957. (b) Gaylord, B. S.; Heeger, A. J.; Bazan, G. C. *J. Am. Chem. Soc.* **2003**, *125*, 896–900. (c) McQuade, D. T.; Hegedus, A. H.; Swager, T. M. *J. Am. Chem. Soc.* **2000**, *122*, 12389–12390. (d) Kim, T. H.; Swager, T. M. *Angew. Chem, Int. Ed.* **2003**, *42*, 4803–4806.

(9) (a) Liu, B.; Bazan, G. C. *Chem. Mater.* **2004**, *16*, 4467–4476. (b) Liu, B.; Bazan, G. C. *J. Am. Chem. Soc.* **2006**, *128*, 1188–1196. (c) Liu, B.; Bazan, G. C. *Proc. Natl. Acad. Sci. U.S.A.* **2005**, *102*, 589–893. (d) He, F.; Tang, Y. L.; Wang, S.; Li, Y. L.; Zhu, D. B. *J. Am. Chem. Soc.* **2005**, *127*, 12343–12346. (e) He, F.; Feng, F. D.; Wang, S.; Li, Y. L.; Zhu, D. B. *J. Mater. Chem.* **2007**, *17*, 3702–3707. (f) Wang, S.; Bazan, G. C. *Adv. Mater.* **2003**, *15*, 1425–1428. (g) Wang, Y. S.; Liu, B. *Chem. Commun.* **2007**, 3553–3555. (h) Wang, Y. S.; Liu, B. *Anal. Chem.* **2007**, *79*, 7214–7220. (i) Liu, B.; Dan, T. T. T.; Bazan, G. C. *Adv. Funct. Mater.* **2007**, *17*, 2432–2438. (j) Liu, B.; Baudrey, S.; Jaeger, J.; Bazan, G. C. *J. Am. Chem. Soc.* **2004**, *126*,

4076–4077. (k) Abérem, M. B.; Najari, A.; Ho, H. A.; Gravel, J. F.; Nobert, P.; Boudreau, D.; Leclerc, M. *Adv. Mater.* **2006**, *18*, 2703–2707. (l) Najari, A.; Ho, H. A.; Gravel, J. F.; Nobert, P.; Boudreau, D.; Leclerc, M. *Anal. Chem.* **2006**, *78*, 7896–7899. (m) Lee, K.; Povlich, L. K.; Kim, J. S. *Adv. Funct. Mater.* **2007**, *17*, 2580–2587. (n) Lee, K.; Rouillard, J. M.; Pham, T.; Gulari, E.; Kim, J. S. *Angew. Chem., Int. Ed.* **2007**, *46*, 4667–4670.

(10) (a) Fan, C. H.; Plaxco, K. W.; Heeger, A. J. *J. Am. Chem. Soc.* **2002**, *124*, 5642–5643. (b) Wang, D. L.; Gong, X.; Heeger, P. S.; Rininsland, F.; Bazan, G. C.; Heeger, A. J. *Proc. Natl. Acad. Sci. U.S.A.* **2002**, *99*, 49–53. (c) Dwight, S. J.; Gaylord, B. S.; Hong, J. W.; Bazan, G. C. *J. Am. Chem. Soc.* **2004**, *126*, 16850–16859. (d) Tan, C. Y.; Atas, E.; Müller, J. G.; Pinto, M. R.; Kleiman, V. D.; Schanze, K. S. *J. Am. Chem. Soc.* **2004**, *126*, 13685–13694. (e) Kim, I. B.; Erdogan, B.; Wilson, J. N.; Bunz, U. H. F. *Chem.—Eur. J.* **2004**, *10*, 6247–6254. (f) Kim, I. B.; Dunkhorst, A.; Gilbert, J.; Bunz, U. H. F. *Macromolecules* **2005**, *38*, 4560–4562.

(11) (a) Ho, H. A.; Leclerc, M. *J. Am. Chem. Soc.* **2003**, *125*, 4412–4413. (b) Ho, H. A.; Leclerc, M. *J. Am. Chem. Soc.* **2004**, *126*, 1384–1387. (c) Zhang, T.; Fan, H. L.; Zhou, J. G.; Liu, G. L.; Feng, G. D.; Jin, Q. H. *Macromolecules* **2006**, *39*, 7839–7843. (d) An, L. L.; Tang, Y. L.; Feng, F. D.; He, F.; Wang, S. *J. Mater. Chem.* **2007**, *17*, 4147–4152.

(12) (a) Hong, J. W.; Henme, W. L.; Keller, G. E.; Rinke, M. T.; Bazan, G. C. *Adv. Mater.* **2006**, *18*, 878–882. (b) Chi, C. Y.; Mikhailovsky, A.; Bazan, G. C. *J. Am. Chem. Soc.* **2007**, *129*, 11134–11145.

(13) (a) Herland, A.; Inganäs, O. *Macromol. Rapid Commun.* **2007**, *28*, 1703–1713. (b) Ambade, A. V.; Sandanaraj, B. S.; Klaikherd, A.; Thayumanavan, S. *Polym. Int.* **2007**, *56*, 474–481. (c) Sandanaraj, B. S.; Demont, R.; Thayumanavan, S. *J. Am. Chem. Soc.* **2007**, *129*, 3506–3507. (d) Zhou, H. C.; Baldini, L.; Hong, J.; Wilson, A. J.; Hamilton, A. D. *J. Am. Chem. Soc.* **2006**, *128*, 2421–2425. (e) Baldini, L.; Wilson, A. J.; Hong, J.; Hamilton, A. D. *J. Am. Chem. Soc.* **2004**, *126*, 5656–5657.

(14) Kim, I. B.; Dunkhorst, A.; Bunz, U. H. F. *Langmuir* **2005**, *21*, 7985–7989.

(15) (a) Zhang, Y.; Cao, Y.; Liu, B. *Chem. Asian J.* **2008**, *3*, 739–745. (b) Pinto, M. R.; Kristal, B. M.; Schanze, K. S. *Langmuir* **2003**, *19*, 6523–6533.

(16) (a) Miranda, O. R.; You, C. C.; Phillips, R.; Kim, I. B.; Ghosh, P. S.; Bunz, U. H. F.; Rotello, V. M. *J. Am. Chem. Soc.* **2007**, *129*, 9856–9857. (b) You, C. C.; Miranda, O. R.; Gider, B.; Ghosh, P. S.; Kim, I. B.; Erdogan, B.; Krovi, S. A.; Bunz, U. H. F.; Rotello, V. M. *Nat. Nanotechnol.* **2007**, *2*, 318–323.

(17) Liu, B.; Gaylord, B. S.; Wang, S.; Bazan, G. C. *J. Am. Chem. Soc.* **2003**, *125*, 6705–6714.

(18) EA results of monomers **1**, **2**, and **3**. **1**: Anal. Calcd for $C_{27}H_{32}Br_2O_4$: C, 55.88; H, 5.56%. Found: C, 55.51; H, 5.53%. **2**: Anal. Calcd for $C_{39}H_{56}Br_2O_8$: C, 69.45; H, 8.37%. Found: C, 69.18; H, 8.38%. **3**: Anal. Calcd for $C_6H_2Br_2N_2S$: C, 24.51; H, 0.69%. Found: C, 24.76; H, 1.14%.

(19) One repeat unit includes one fluorene moiety and relevant content of BT. The molecular weight of the RUs are (0.925 substituted fluorene + 0.075 BT = 0.925 × 352.31 + 0.075 × 136.17 = 336.1) 336.1 g/mol, (0.85 substituted fluorene + 0.15 BT = 0.85 × 352.31 + 0.15 × 136.17 = 319.9) 319.9 g/mol, and (0.70 substituted fluorene + 0.30 BT = 0.70 × 352.31 + 0.30 × 136.17 = 287.5) 287.5 g/mol for **P2-BT$_{7.5}$**, **P2-BT$_{15}$**, and **P2-BT$_{30}$**, respectively.

(20) (a) Herguch, P.; Jiang, X. Z.; Liu, M. S.; Jen, A. K. Y. *Macromolecules* **2002**, *35*, 6094–6100. (b) Huang, F.; Hou, L. T.; Wu, H. B.; Yang, X. H.; Shen, H. L.; Cao, W.; Yang, W.; Cao, Y. *J. Am. Chem. Soc.* **2004**, *126*, 9485–9853. (c) Yang, R. Q.; Tian, R. Y.; Hou, Q.; Yang, W.; Cao, Y. *Macromolecules* **2003**, *36*, 7453–7460.

(21) Liu, B.; Yu, W. L.; Lai, Y. H.; Huang, W. *Chem. Mater.* **2001**, *13*, 1984–1991.

(22) (a) Kim, B. S.; Chen, L.; Gong, J. P.; Osada, Y. *Macromolecules* **1999**, *32*, 3964–3969. (b) Kawaguchi, S.; Nishikawa, Y.; Kitano, T.; Ito, K.; Minakata, A. *Macromolecules* **1990**, *23*, 2710–2714.

(23) Brookins, R. N.; Schanze, K. S.; Reynolds, J. R. *Macromolecules* **2007**, *40*, 3524–3526.

(24) (a) Kawaguchi, K.; Kitano, T.; Ito, K. *Macromolecules* **1991**, *24*, 6030–6036. (b) Kawaguchi, K.; Kitano, T.; Ito, K. *Macromolecules* **1992**, *25*, 1294–1299.

(25) Henry, B. R.; Morrison, J. D. *J. Mol. Spectrosc.* **1975**, *55*, 311–318. (b) Lin, T. S.; Braun, J. R. *Chem. Phys.* **1978**, *28*, 379–386. (c) Lim, E. C. *J. Phys. Chem.* **1986**, *90*, 6770–6777.

(26) Wang, F. K.; Bazan, G. C. *J. Am. Chem. Soc.* **2006**, *128*, 15786–15792.

(27) (a) Israelachvili, J. *Intermolecular & Surface Forces*; Academic Press: London, 1992. (b) Zhang, Y.; Milam, V. T.; Graves, D. J.; Hammer, D. A. *Biophys. J.* **2006**, *90*, 4128–4136.

(28) Mandel, M.; Leyte, J. C. *J. Polym. Sci.* **1962**, *56*, S23—S25.

(29) Zunszain, P. A.; Ghuman, J.; Komatsu, T.; Tsuchida, E.; Curry, S. *BMC Struct. Biol.* **2003**, *3*, 6–10.

(30) Pepys, M. B.; Hawkins, P. N.; Booth, D. R.; Vigushin, D. M.; Tennent, G. A.; Soutar, A. K.; Totty, N.; Nguyen, O.; Blake, C. C. F.; Terry, C. J.; Feest, T. G.; Zalin, A. M.; Hsuan, J. J. *Nature (London)* **1993**, *362*, 553–557.

(31) Chen, Y. M.; Yu, C. J.; Cheng, T. L.; Tseng, W. L. *Langmuir* **2008**, *24*, 3654–3660.

MA800082K